

J. A. Weil, J. R. Bolton, and J. E. Wertz, *op. cit.*

A useful compilation of EPR data is J. A. Pedersen, *Handbook of EPR Spectra from Quinones and Quinols*, CRC Press, Boca Raton, Fla. (1985).

EXPERIMENT 42

NMR Determination of Keto-Enol Equilibrium Constants

In this experiment, proton NMR spectroscopy is used in evaluating the equilibrium composition of various keto-enol mixtures. Chemical shifts and spin-spin splitting patterns are employed to assign the spectral features to specific protons, and the integrated intensities are used to yield a quantitative measure of the relative amounts of the keto and enol forms. Solvent effects on the chemical shifts and on the equilibrium constant are investigated for one or more β -diketones and β -ketoesters.

THEORY

Chemical Shifts. In Exp. 33, the Zeeman energy levels of a nucleus in an external applied field were given as

$$E_N = -g_N \mu_N M_I B_{\text{loc}} \quad (1)$$

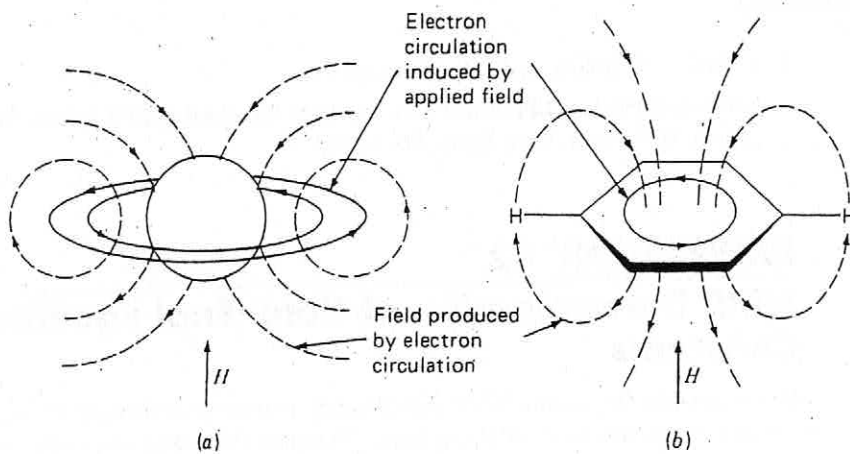
where B_{loc} is the magnetic induction ("local field") at the nucleus. As a result of the $\Delta M_I = \pm 1$ selection rule, a transition will occur at frequency

$$\nu_i = \left(\frac{g_N \mu_N}{h} \right) B_{i,\text{loc}} \quad (2)$$

for a nucleus i . The chemical shift in parts per million (ppm) of this nucleus relative to a reference nucleus r is defined by

$$\delta_i \equiv \frac{\nu_i - \nu_r}{\nu_r} \times 10^6 = \frac{B_r - B_i}{B_r} \times 10^6 \quad (3)$$

Here the first definition is based on the resonant frequencies for a fixed external induction (field) B , whereas the second (nearly equivalent) relation is based on the more common experimental case where B is varied to achieve resonance at a fixed instrumental frequency ν . Tetramethylsilane (TMS) is usually used as the proton reference, since it is chemically inert and its 12 equivalent protons give a single transition at a field B_r , higher than the field B_i found in most organic compounds. Thus δ is generally positive and increases when substituents are added that attract electrons and thereby reduce the shielding about the proton. This shielding arises because the electrons near the proton are induced to circulate by the applied field B (see Fig. 1a). This electron current produces a secondary field that *opposes* the external field and thus reduces the local field at the proton. As a result, resonance at a fixed frequency such as 60 MHz requires a higher external field for protons with larger shielding. This shielding effect is generally restricted to electrons localized on the nucleus of interest, since random tumbling of the molecules causes the effect of secondary fields due to electrons associated with neighboring nuclei to average to zero. Nuclei such as ^{19}F , ^{13}C , and ^{11}B have more local electrons than hydrogen, hence their chemical shifts are much larger.

**FIGURE 1**

Shielding and deshielding of protons: (a) shielding of proton due to induced diamagnetic electron circulation; (b) Deshielding of protons in benzene due to aromatic ring currents.

Long-range *deshielding* can occur in aromatic and other molecules with delocalized π electrons. For example, when the plane of the benzene molecule is oriented perpendicular to B , circulation of the π electrons produces a ring current (see Fig. 1b). This ring current induces a secondary field at the protons that is *aligned parallel* to B and thus increases the local field at the protons. This induced field changes with benzene orientation but does not average to zero, since it is not spherically symmetric. Because of this net deshielding effect, the resonance of the benzene protons occurs at a relatively low external field. The proton chemical shift δ for benzene is 7.27, greatly downfield from the value $\delta = 1.43$ that is observed for cyclohexane, in which ring currents do not occur. Similar deshielding occurs for olefinic and aldehydic protons because of the π electron movement. Typical values of δ for different functional groups are shown in Table 1, and additional values are available in Refs. 1 to 3. Although the resonances change somewhat for different compounds, the range for a given functional group is usually small and δ values are widely used for structural characterization in organic chemistry.

TABLE 1 Typical proton chemical shifts δ

| CH_3 protons | | Acetylenic protons | |
|--|------|--|------|
| $(\text{CH}_3)_4\text{Si}$ | 0.0 | $\text{HOCH}_2\text{C}\equiv\text{CH}$ | 2.33 |
| $(\text{CH}_3)_4\text{C}$ | 0.92 | $\text{ClCH}_2\text{C}\equiv\text{CH}$ | 2.40 |
| $\text{CH}_3\text{CH}_2\text{OH}$ | 1.17 | $\text{CH}_3\text{COC}\equiv\text{CH}$ | 3.17 |
| CH_3COCH_3 | 2.07 | Olefinic protons | |
| CH_3OH | 3.38 | $(\text{CH}_3)_2\text{C}=\text{CH}_2$ | 4.6 |
| CH_3F | 4.30 | Cyclohexane | 5.57 |
| CH_2 protons | | $\text{CH}_3\text{CH}=\text{CHCHO}$ | 6.05 |
| Cyclopropane | 0.22 | $\text{Cl}_2\text{C}=\text{CHCl}$ | 6.45 |
| $\text{CH}_3(\text{CH}_2)_4\text{CH}_3$ | 1.25 | Aromatic protons | |
| $(\text{CH}_3\text{CH}_2)_2\text{CO}$ | 2.39 | Benzene | 7.27 |
| $\text{CH}_3\text{COCH}_2\text{COOCH}_3$ | 3.48 | $\text{C}_6\text{H}_5\text{CN}$ | 7.54 |
| $\text{CH}_3\text{CH}_2\text{OH}$ | 3.59 | Naphthalene | 7.73 |
| CH protons | | α -Pyridine | 8.50 |
| Bicyclo[2.2.1]heptane | 2.19 | Aldehydic protons | |
| Chlorocyclopropane | 2.95 | CH_3OCHO | 8.03 |
| $(\text{CH}_3)_2\text{CHOH}$ | 3.95 | CH_3CHO | 9.72 |
| $(\text{CH}_3)_2\text{CHBr}$ | 4.17 | $\text{C}_6\text{H}_5\text{CHO}$ | 9.96 |

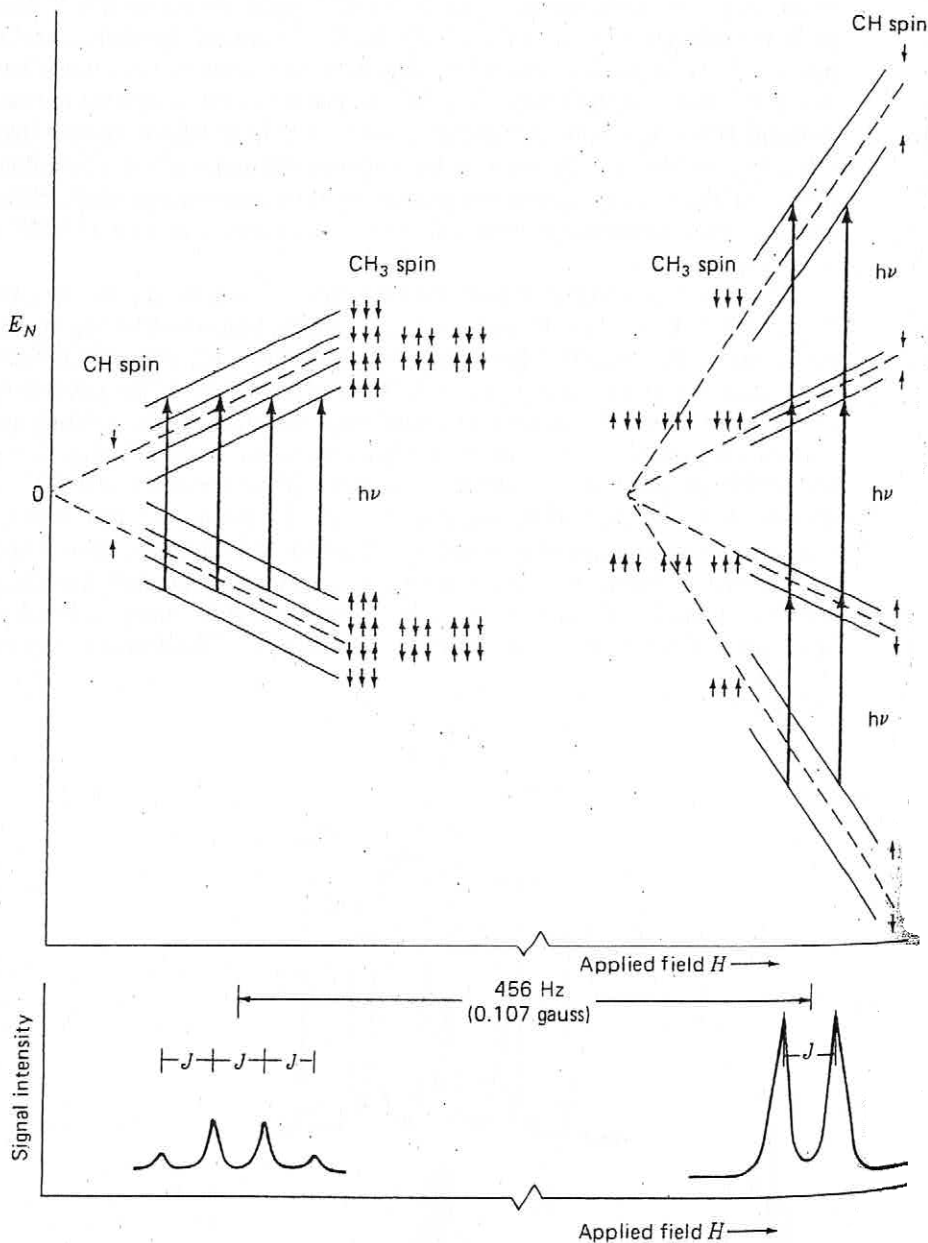
Spin-Spin Splitting. High-resolution NMR spectra of most organic compounds reveal more complicated spectra than those predicted by Eq. (2), with transitions often appearing as multiplets. Such *spin-spin splitting patterns* arise because the magnetic moment of one proton (A) can interact with that of a nearby nucleus (B), causing a small energy shift up or down depending on the relative orientations of the two moments. The energy levels of nucleus A then have the form

$$E_A = -g_N \mu_N M_{I_A} (1 - \sigma_A) B + hJ_{AB} M_{I_A} M_{I_B} \quad (4)$$

and there is a similar expression for E_B . The spin-spin interaction is characterized by the coupling constant J_{AB} , and the effect is to split the energy levels in the manner illustrated for acetaldehyde in Fig. 2. It is apparent from this diagram that the external field B does

FIGURE 2

Energy levels, transitions, and 60-MHz NMR spectrum for acetaldehyde (CH_3CHO). The coupling constant $J = J_{\text{CH}_3} = J_{\text{CH}} = 2.2 \text{ Hz}$ ($= 5.2 \times 10^{-4} \text{ gauss} = 5.2 \times 10^{-8} \text{ T}$). For CH, the quantum number $M_J = -\frac{1}{2}$ or $\frac{1}{2}$. For the CH_3 group, $M_J = -\frac{3}{2}, -\frac{1}{2}, +\frac{1}{2}, +\frac{3}{2}$. The dashed lines represent the level spacing that would occur in the absence of the spin-spin interaction. The slopes of the energy levels are greatly exaggerated in the figure. Also, to be correct, all dashed lines should extrapolate to a common $E_N = 0$ at $H = 0$.



not effect the small spin-spin splitting that is characterized by the coupling constant J . The quantity J is a measure of the strength of the pairwise interaction of the proton spin with the spin of another nucleus. Since there are only proton-proton interactions in acetaldehyde, the same splitting occurs for both CH and CH_3 resonances.

The total integrated intensity of the CH and CH_3 multiplets follows the proton ratio of 1:3. However, the intensity distribution within each multiplet is determined by the relative population of the lower level in each transition. Since the level spacing is much less than kT , the Boltzmann population factors are essentially identical for these levels. However, there is some degeneracy because rapid rotation of the CH_3 group around the C-C bond makes the three protons magnetically equivalent. The number of spin orientations of the CH_3 protons that produce equivalent fields at the CH proton determine the degeneracy. The eight permutations of the CH_3 spins shown in Fig. 2 thus lead to a predicted intensity ratio of 1:3:3:1 for the CH multiplet. Similarly, the CH_3 doublet peaks will be of equal intensity, with a total integrated intensity three times that of the CH peaks. In a more general sense, it can be seen that n equivalent protons interacting with a different proton will split its resonance into $n + 1$ lines whose relative intensities are given by coefficients of the terms in the binomial expansion of the expression $(\alpha + \beta)^n$. Equivalent protons also interact and produce splitting in the energy levels. However, these splittings are symmetric for upper and lower energy states, so no new NMR resonances are produced.

If a proton is coupled to more than one type of neighboring nucleus, the resultant multiplet pattern can often be understood as a simple stepwise coupling involving different J values. For example, the CH_2 octet that occurs for pure $\text{CH}_3\text{CH}_2\text{OH}$ (Fig. 3) arises from OH doublet splitting ($J = 4.80$ Hz) of the quartet of lines caused by coupling ($J = 7.15$ Hz) with CH_3 . It should be mentioned that such regular splitting and intensity patterns are expected for two nuclei A and B only if $|\nu_A - \nu_B| \geq 10J_{AB}$. The spectra for this weakly coupled case are termed *first-order*. Since the difference $\nu_A - \nu_B$ (in Hz) increases with the field while J_{AB} does not, NMR spectra obtained with a high-field instrument (400 MHz) are often easier to interpret than those from a low-field spectrometer (60 MHz). However, even if the multiplets are not well separated, it is still possible to deduce accurate chemical shifts and J values using slightly more involved procedures, which are outlined in most texts on NMR spectroscopy.¹⁻⁵ Such an exercise can be done

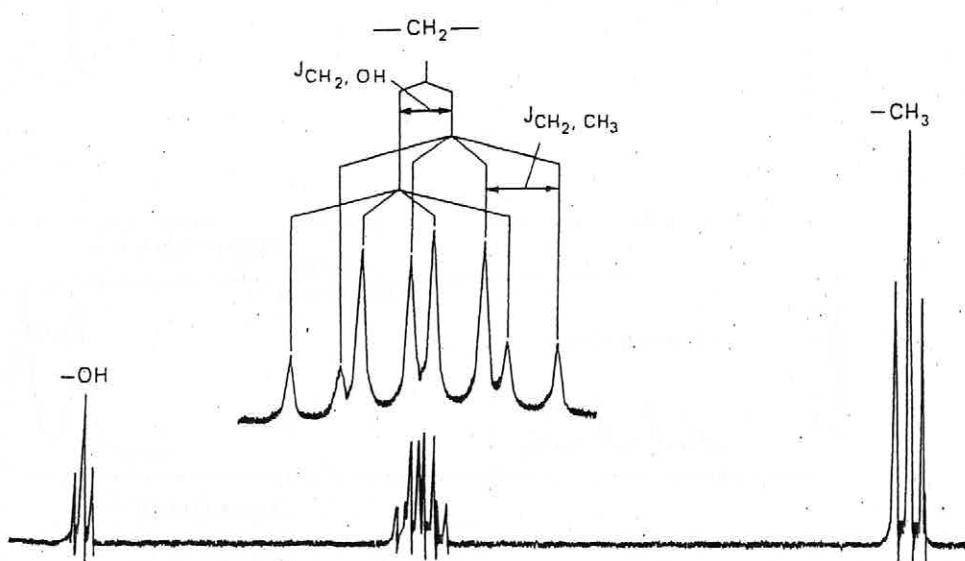
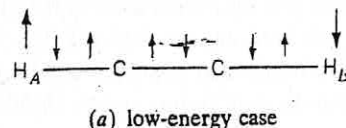


FIGURE 3
NMR spectrum of highly purified ethanol obtained at 100 MHz.

FIGURE 4

Illustration of nuclear spin-spin interaction transmitted via polarization of bonding electrons. The two electrons about each carbon will tend to be parallel, since this arrangement minimizes the electron-electron repulsion (Hund's rule for electrons in degenerate orbitals).



as an optional part of this experiment, although it will not be necessary for the determination of equilibrium constants.

The mechanism of spin-spin coupling is known to be indirect and to involve the electrons in the bonds between interacting nuclei. The spin of the first nucleus A is preferentially coupled antiparallel to the nearest bonding electron via the so-called Fermi contact interaction, which is significant only when the electron density is nonzero at the first nucleus. (Such is the case only for electrons in *s* orbitals, since *p*, *d*, and *f* orbital wavefunctions have zero values at the nucleus.) This electron-spin alignment information is transmitted by electron-electron interactions to the second nucleus B to produce a field which thus depends on the spin orientation of the first nucleus (Fig. 4). Since the strength of this interaction falls rapidly with separation, only neighboring groups produce significant splitting. A few typical spin-spin coupling constants are given in Table 2 and these, along with the chemical shifts, serve to identify proton functional groups. As mentioned above, the multiplet intensities also give useful information about neighboring groups. Thus NMR spectra can provide detailed structural information about large and complex molecules.

Keto-Enol Tautomerism. It is well known that ketones such as acetone have an isomeric structure, which results from proton movement, called the enol tautomer, an unsaturated alcohol:

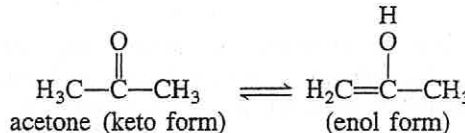
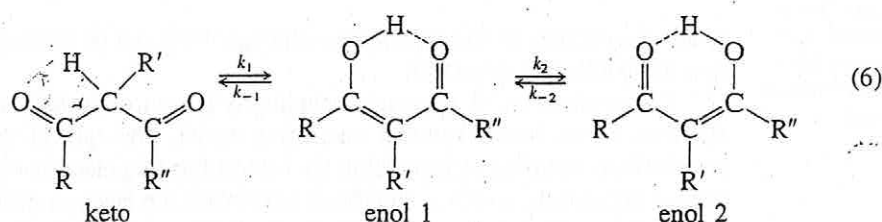


TABLE 2 Typical proton spin-spin coupling constants

| COUPLING | <i>J</i> (Hz) | COUPLING | <i>J</i> (Hz) |
|---|---------------|---|---------------|
|  | -20 to +5 |  | 0 to 3.5 |
|  | 2 to 9 |  | 6 to 14 |
|  | 0 | | |
|  | 6 to 9 |  | 11 to 19 |
| <i>meta-</i> <i>para-</i> | 1 to 3 |  | |
| | 1 | | |

For acetone, and the majority of cases in which this keto-enol tautomerism is possible, the keto form is far more stable and little if any enol can be detected. However, with β -diketones and β -ketoesters, such factors as intramolecular hydrogen bonding and conjugation increase the stability of the enol form and the equilibrium can be shifted significantly to the right.



The proton chemical environments are quite different for the keto and enol tautomers, and the interconversion rate constants k_1 and k_{-1} between these forms are small enough that distinct NMR spectra are obtained for both forms. In principle, the two enols are also distinguishable when $R' \neq R''$. However, the intramolecular OH proton transfer is quite rapid at normal temperatures, so that a single (average) OH resonance is observed. In general, such averaging occurs when the conversion rates k_2 and k_{-2} (in Hz) exceed the frequency separation $\nu_1 - \nu_2$ (also in Hz) of the OH resonance for the two enol forms.² The magnetic field at the OH proton is thus averaged and resonance occurs at $(\nu_1 + \nu_2)/2$. Similarly, rapid rotation about the C—C bonds of the keto form explains why spectra due to different keto rotational conformers are not observed. Thus, distinct spectra are expected only for the two tautomers, and these can be used to determine the equilibrium constant for keto-to-enol conversion:

$$K_c = \frac{(\text{enol})}{(\text{keto})} \quad (7)$$

where parentheses denote concentrations in any convenient units.

The keto arrangement shown in Eq. (6) is the configuration which is electrostatically most favorable, but the steric repulsions between R and R" groups will be larger for this keto form than for the enol configuration. Indeed, experimental studies have confirmed that the enol concentration is larger when R and R" are bulky.⁴ This steric effect is less important in the β -ketoesters, in which the R···R" separation is greater. For both β -ketoesters and β -diketones, α substitution of large R' groups results in steric hindrance between R' and R (or R") groups, particularly for the enol tautomer, whose concentration is thereby reduced. Inductive effects have also been explored; in general, α substitution of electron-withdrawing groups such as —Cl or —CF₃ favor the enol form.⁴

The solvent plays an important role in determining K_c . This can occur through specific solute-solvent interactions such as hydrogen bonding or charge transfer. In addition, the solvent can reduce solute-solute interactions by dilution and thereby change the equilibrium if such interactions are different in enol-enol, enol-keto, or keto-keto dimers. Finally, the dielectric constant of the solution will depend on the solvent and one can expect the more polar tautomeric form to be favored by polar solvents. Some of these aspects are explored in this experiment.

EXPERIMENTAL

The general features of a CW NMR spectrometer were described briefly in Exp. 33, and details about Fourier-transform NMR instruments are given in Exp. 43. For the

spectrometer you are to use, more specific operating instructions will be provided by the instructor. Obtain a milliliter each of acetylacetone ($\text{CH}_3\text{OCH}_2\text{COCH}_3$, M.W. = 100.11, density = 0.98 g cm^{-3}) and ethyl acetoacetate ($\text{CH}_3\text{CH}_2\text{OCOCH}_2\text{COCH}_3$, M.W. = 130.45, density = 1.03 g cm^{-3}). Prepare small volumes of two solvents and three solutions.

Solvent A: deuterated chloroform, spectrochemical grade (M.W. = 120.38, density = 1.50 g cm^{-3})

Prepare in a 1.5 or 2.0mL microfuge tube.

Solvent B: d4-Methanol, spectrochemical grade (M.W. = 36.07, density = 0.888 g cm^{-3})

Prepare in a

1.5 or 2.0mL microfuge tube.

Solution 1: 0.05 mole fraction of acetylacetone in solvent A

Solvent 2: 0.05 mole fraction of acetylacetone in solvent B

Solution 3: 0.05 mole fraction of ethyl acetoacetate in solvent A

Use a 100 μL micropipettor to measure out 0.0005 mol of solute, and use a 1000 μL micropipettor to then add the correct amount (0.0095) of solvent.

Record the NMR spectra

for solutions 1 to 3, taking care to scan above $\delta = 16$ ppm since the enol OH peak is shifted substantially downfield. Determine which peaks are due to solute and measure chemical shifts for all solute features. Integrate the bands carefully, expanding the vertical scale in order to obtain accurate relative intensity measurements.

CALCULATIONS

Assign all spectral features using Table 1 and other NMR reference sources.^{2,3,5} Tabulate your results and use your integrated intensities to calculate the percentage enol present in solutions 1 to 3. If possible, use the total integral corresponding to the sum of methyl (or ethyl), methylene, methyne, and enol protons. If this proves difficult because of overlap with solvent bands, indicate clearly how you used the intensities to calculate the percentage enol.

For both the enol and the keto forms, compare experimental and theoretical ratios of the integrated intensities for different types of protons (e.g., methyl to methylene protons in the keto form).

Using Eq. (7), calculate K_c and the corresponding standard free-energy difference ΔG^0 for the change in state keto \rightarrow enol in each solution.

DISCUSSION

Discuss briefly your assignments of chemical shifts and spin–spin splitting patterns of acetylacetone and ethyl acetoacetate. Which compound has a higher concentration of enol form, and what reasons can you offer to explain this result? What changes would you expect in the NMR spectra of these two compounds if the interconversion rate between enol structures were much slower?

Compare the value of K_c for acetylacetone in CDCl_3 with that in CD_3OD . What does

your result suggest regarding the relative polarity of the enol and keto forms? Which form is favored by hydrogen bonding and why?

Compare your values of ΔG^0 with those for the gas phase ($\Delta G^0 = -9.2 \pm 2.1 \text{ kJ mol}^{-1}$ for acetylacetone, $\Delta G^0 = -0.4 \pm 2.5 \text{ kJ mol}^{-1}$ for ethyl acetoacetate).⁶ What solvent properties might account for any differences you observe?

Additional compounds suitable for studies of steric effects on keto-enol equilibria include α -methylacetone ($\text{CH}_3\text{COCHCH}_3\text{COCH}_3$), diethylmalonate ($\text{CH}_3\text{CH}_2\text{OCOCH}_2\text{COOCH}_2\text{CH}_3$), ethyl benzoylacetate ($\text{C}_6\text{H}_5\text{COCH}_2\text{COOCH}_2\text{CH}_3$), and *t*-butyl acetoacetate ($\text{CH}_3\text{COCH}_2\text{COOt-Bu}$). Some other possible compounds are listed in Refs. 4 and 5. Further aspects of this equilibrium that could be studied include the effects of concentration, temperature, and solvent dielectric constants on K_c .⁵

SAFETY ISSUES

None of these chemicals are significantly toxic. Standard laboratory precautions should be followed.

APPARATUS

NMR spectrometer with integrating capability; microfuge tubes,
100 μL and 1000 μL micropipettors, NMR tubes; spectrochemical-grade CDCl_3 and CD_3OD ; acetylacetone, and ethyl acetoacetate.

REFERENCES

1. J. C. Davis, Jr., *Advanced Physical Chemistry: Molecules, Structure, and Spectra*, Wiley-Interscience, New York (1965).
2. J. A. Pople, W. G. Schneider, and H. J. Bernstein, *High Resolution Nuclear Magnetic Resonance*, McGraw-Hill, New York (1959); C. P. Slichter, *Principles of Magnetic Resonance*, 2d ed., vol I in P. Fulde (ed.), *Solid State Sciences*, Springer-Verlag, Berlin/New York (1980).
3. Compilations of NMR chemical shifts and coupling constants are given in F. A. Bovey, *NMR Data Tables for Organic Compounds*, vol. I, Wiley-Interscience, New York (1967), and in L. F. Johnson and W. C. Jankowski, *C-13 NMR Spectra*, Wiley-Interscience, New York (1972).
4. J. L. Burdett and M. T. Rogers, *J. Amer. Chem. Soc.* **86**, 2105 (1964).
5. M. T. Rogers and J. L. Burdett, *Can. J. Chem.* **43**, 1516 (1965).
6. M. M. Folkendt, B. E. Weiss-Lopez, J. P. Chauvel, Jr., and N. S. True, *J. Phys. Chem.* **89**, 3347 (1985).

GENERAL READING

- R. J. Abraham, J. Fisher, and P. Lofthus, *Introduction to NMR Spectroscopy*, Wiley, New York (1991).
- R. Drago, *Physical Methods for Chemists*, 2d ed., chaps. 7, 8, Saunders, Philadelphia (1992).
- R. K. Harris, *Nuclear Magnetic Resonance Spectroscopy*, Longman, London (1986).
- C. P. Slichter, *op. cit.*

1.2.2. NMR experiments

1.2.2.1. NMR sample preparation

Delipidated fractions containing LFABP were pooled, concentrated and exchanged into the buffer (100 mM KCl, 50 mM KH₂PO₄, 5 μM EDTA, 0.02% NaN₃, pH 7.0) conventionally used for NMR experiments. The desired concentrations for acquisition of two-dimensional (HSQC) and three-dimensional (TOCSY-HSQC, NOESY-HSQC) NMR spectrum are in the range of 0.1-0.3 mM and 0.4-0.8 mM respectively. Concentration was determined using Nanodrop (Wilmington, DE) with 6400 M⁻¹ cm⁻¹ as the absorption coefficient of LFABP⁷. 5% by volume D₂O was added to 500 μl NMR sample for a ²H lock signal and it was put into a 5mm NMR tube.

1.2.2.2. 2D ¹⁵N HSQC

¹⁵N-HSQC spectra were recorded using a Varian four-channel spectrometer with ¹H frequency at 600 MHz (conventional probe). In specific cases, a Varian instrument with cryoprobe was also used. Alternatively, a Bruker four-channel spectrometer with cryoprobe was used. ¹⁵N-HSQC spectra were recorded with 1024 points in the direct dimension, 256 points in the indirect dimension and with 32 transients, unless otherwise mentioned. The data were processed with NMRpipe software²⁰, with typical parameters as shown in Table 1.1 and analyzed with NMRView²¹.

| | |
|--|---------------------------|
| nmrPipe -in test.fid | .Format Input |
| nmrPipe -fn SOL -fl 32 | solvent filter |
| nmrPipe -fn SP -off 0.35 -end 1.00 -pow 2 -c 0.5 | Window |
| nmrPipe -fn ZF -auto | Zero-fill |
| nmrPipe -fn FT -auto | Fourier-transform |
| nmrPipe -fn PS -p0 41.00 -p1 0.00 -di -verb | Phase, delete imaginaries |

| | |
|--|--|
| nmrPipe -fn POLY -auto -ord 0 | <i>Auto-baseline correct</i> |
| nmrPipe -fn EXT -left -sw | <i>Extract the left half</i> |
| nmrPipe -fn TP | <i>Transpose X/Y</i> |
| nmrPipe -fn LP -x1 1 -xn 64 -ord 10 -f -pred 64 -after | <i>Linear prediction</i> |
| nmrPipe -fn SP -off 0.35 -end 1.00 -pow 2 -c 0.5 | <i>Window</i> |
| nmrPipe -fn ZF -auto | <i>Zero-fill</i> |
| nmrPipe -fn FT -alt | <i>Fourier transform</i> |
| nmrPipe -fn PS -p0 0.0 -p1 0.00 -di -verb | <i>Phase correct, delete imaginaries</i> |
| nmrPipe -fn TP | <i>Transpose X/Y</i> |
| nmrPipe -fn POLY -auto -ord 0 | <i>Auto-baseline correct</i> |
| -ov -out test.dat | <i>Format output</i> |

Table 1.1. Annotated conversion script used for HSQC spectrum recorded in Bruker 500 spectrometer at pH 7.0, 283K.

1.2.2.3. Double resonance experiments and NMR assignment of LFABP

a) Three-dimensional TOCSY-HSQC and NOESY-HSQC

TOCSY-HSQC and NOESY-HSQC data were acquired for confirming backbone resonance assignments of apo and oleate liganded holo-LFABP with 1024 complex points in t_1 , 256 complex points in t_2 and 128 complex points in t_3 . 32 transients were acquired using a four-channel Bruker 500 MHz spectrometer with a cryoprobe. Similar experiments were recorded for backbone resonance assignments of the warfarin-oleate-LFABP complex.

1.2.2.4. Titration followed by NMR

^{15}N -HSQC experiments were recorded with sequential addition of specific ligand solutions (oleate, linoleate) into apo-LFABP at 10°C. Typically, aliquots of a 2 mM stock solution of sodium oleate at pH 9.0 were added to 0.14 mM apo-LFABP in 100 mM KCl, 50 mM KH_2PO_4 , 5 μM EDTA, 0.02% NaN_3 , pH 7.0 buffer. The titration points recorded were 1:0.26, 1:0.5, 1:0.65, 1:0.78, 1:0.9, 1:1.16, 1:1.68, 1:1.95, 1:2.97 and 1:4 equivalent of protein: ligand. At the end of

the titration series, the dilution factor was 1.13 times owing to the addition of aliquots of ligand solution.

In case of linoleate, a pH 9.0, 1 mM stock solution was used and the titration points recorded were 1:0.08, 1:0.17, 1:0.25, 1:0.42, 1:0.6, 1:0.77, 1:0.94, 1:1.3, 1:1.6, 1:1.97, 1:2.5, 1:3 with similar pH and temperature as oleate. At the end of the titration series the dilution factor was 1.12 times owing to the addition of aliquots of ligand solution.

For warfarin, the titration series presented herein, started with holo-LFABP liganded with 2 equivalents of oleate. 10 mM warfarin dissolved in sodium hydroxide was used to record 0.4, 0.8, 1.2, 1.6, and 2 equivalents of added warfarin to holo-LFABP complex.

For a trial with phytanic acid, starting with apo-LFABP, 3 equivalents were added from 5mM solution of isomers of phytanic acid in NaOH and HSQC spectrum was recorded.

For glucose, excess of glucose (10 equivalents) 10 mM solution was added to apo-LFABP and HSQC spectrum was recorded.

1.2.2.5. Chemical shift perturbation analysis

Upon sequential addition of ligand solution to ^{15}N -LFABP NMR samples, the HSQC peaks of certain residues of the apo-protein spectrum may be perturbed due to a change in the chemical environment as a consequence of the interaction of the protein with the ligand. This chemical shift perturbation (in ppm) was calculated using the formula $[(\delta_{\text{Hapo}} - \delta_{\text{Hholo}})^2 + \{(\delta_{\text{Napo}} - \delta_{\text{Nholo}})/6.51\}^2]^{1/2}$, where δ_{H} is the proton chemical shift, whereas δ_{N} is the nitrogen chemical shift²².